

The γ -ray emission in the region of W49A with *Fermi*-LAT

Yu-Liang Xin^{a,*} and Xiao-Lei Guo^a

^a*School of Physical Science and Technology, Southwest Jiaotong University, Chengdu 610031, China*

E-mail: ylxin@swjtu.edu.cn, xlguo@swjtu.edu.cn

The young star clusters/star forming regions have been believed to be the Galactic CRs contributors. As the CR acceleration sites, the collective effect of stellar winds and/or supernova activity in the young stellar associations can produce a large-scale shock, which will accelerate the particles up to energies of hundreds of TeV. W49A is one of the massive and luminous star forming region in the Galaxy and one of the richest clusters known. Using the *Fermi*-LAT Pass 8 data, here we report the detection of the γ -ray emission around W49A.

37th International Cosmic Ray Conference (ICRC 2021)
July 12th – 23rd, 2021
Online – Berlin, Germany

*Presenter

1. Introduction

It is widely believed that supernova remnants (SNRs) are the dominant accelerators of Galactic cosmic rays (CRs) with energies up to the knee. The electrons and protons can be accelerated to be the ultra-relativistic particles by the shock of SNRs via the diffusive shock acceleration mechanism. The high-energy electrons can produce the radio/non-thermal X-ray emission by synchrotron radiation and the γ -ray emission by the inverse Compton scattering (ICS)/bremsstrahlung process (leptonic process). The γ -ray emission of SNRs also can be from the decay of neutral pions produced by inelastic proton-proton collisions (hadronic process).

In recent years, a large number of γ -ray sources including SNRs have been detected by *Fermi* Large Area Telescope (*Fermi*-LAT) and the ground-based γ -ray telescopes, like HESS, VERITAS, MAGIC, etc. Meanwhile, these observations also reveal several new classes of γ -ray sources and some of them may also provide the non-negligible contribution to the Galactic CRs. One kind of the γ -ray sources is the young star cluster in the star forming region. As the CR acceleration sites, the collective effect of stellar winds and/or supernova activity in the young stellar associations can produce a large-scale shock, which will accelerate the particles up to energies of hundreds of TeV [1, 2]. And these high-energy particles can produce the multi-wavelength emission by the different radiation mechanisms, especially through the hadronic interactions between the relativistic particles and the dense interstellar mediums in the star clusters. And the GeV or TeV γ -ray emission from such sources has been detected, like Cygnus Cocoon [3], Westerlund 1 [4], and NGC 3603 [5], etc.

The W49 region is one of the most interacting regions in the Galaxy to study the CR acceleration and it contains a star forming region W49A and a young SNR W49B. W49B is a SNR which is interacting with the molecular clouds and its distance is estimated to be ~ 10 kpc by Zhu et al. [6]. The γ -ray emission of W49B has been detected by *Fermi*-LAT and HESS [7, 8].

W49A, located 0.21° to the west of the SNR W49B, is one of the massive ($\sim 10^6 M_\odot$) and luminous ($>10^7 L_\odot$) star forming region in the Galaxy and one of the richest clusters known [9]. W49A contains numerous compact/ultracompact HII regions and its luminosity is a result of an embedded stellar cluster containing the equivalent of about 100 O7 stars [10, 11]. The distance of W49A is determined to be $11.11^{+0.79}_{-0.69}$ kpc by Zhang et al. [12]. Several works have been done trying to search for the γ -ray emission from W49A using the data of *Fermi*-LAT and HESS [7, 8] and only upper limits are gotten. It should be noted that H. E. S. S. Collaboration et al. [8] reported a signal of the TeV γ -ray emission from W49A, but it is too weak ($<5\sigma$) to do the further analysis. Here, we will report the detection of the γ -ray emission around W49A, with the Pass 8 data recorded by the *Fermi*-LAT.

2. *Fermi*-LAT Data Reduction

In the following data analysis, the *Fermi*-LAT data with ‘‘Source’’ event class are selected, collected from 2008 August 4 (MET 239557418) to 2021 January 4 (MET 631411205). The energy range adopted is 1 GeV - 1 TeV, and the maximum zenith angle is 90° to reduce the contamination from the Earth Limb. The region of interest (ROI) is a square region of $14^\circ \times 14^\circ$ centered at the position at 4FGL J1910.2+0904c, a point source in the fourth *Fermi*-LAT source catalog [13], which is positionally coincident with W49A. The data are analyzed using standard LAT

analysis software *Fermitools* with the instrument response function (IRF) of “P8R3_SOURCE_V2”. The Galactic and isotropic diffuse background emissions are modeled by `gll_iem_v07.fits` and `iso_P8R3_SOURCE_V2_v1.txt`, respectively. The binned likelihood method is adopted, and all sources listed in the 4FGL catalog within a radius of 20° from the ROI center are included in the model.

3. Analysis and Results

With the 4FGL source model, we first created a test statistic (TS) map by subtracting the γ -ray emissions from the sources and backgrounds in the best-fit model with *gtsmap*, which is shown in the left panel of Figure 1. Some residual emissions are shown in this TS map, and we added two new point sources (R.A.= 287.99° , Dec.= 9.05° and R.A.= 287.88° , Dec.= 9.80°) in the model with the power-law spectra. Then, we adopted the position of 4FGL J1910.2+0904c (positionally coincident with W49A) provisionally provided in the 4FGL catalog to get the spectrum of it. The data were binned into ten equal logarithmic energy bins from 1 GeV to 1 TeV. For each energy bin, the same likelihood fitting is adopted, and the upper limits with 95% confidence level are calculated for the TS value of 4FGL J1910.2+0904c smaller than 4.0. The resulting spectral energy distribution (SED) is shown in the right panel of Figure 1, and there is an obvious spectral upturn at an energy of about 20 GeV.

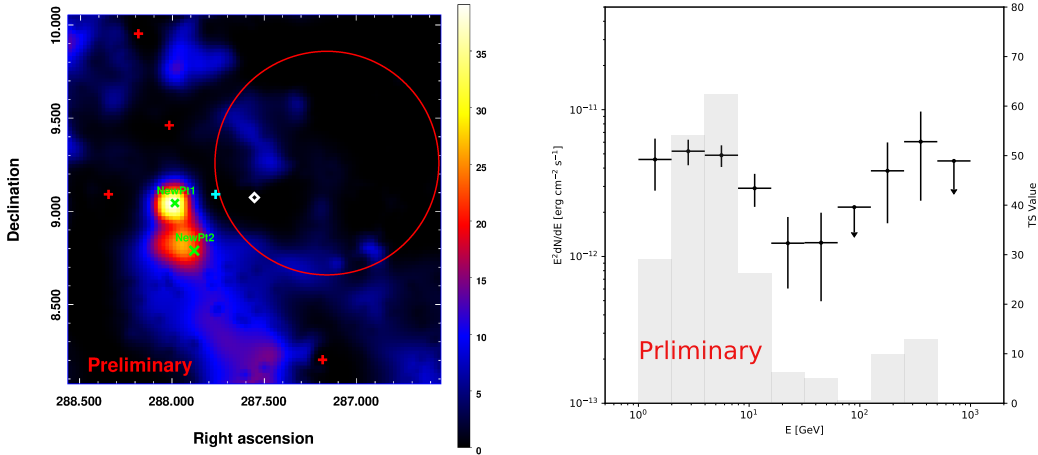


Figure 1: Left: TS map of a $2^\circ \times 2^\circ$ region. The red pluses are the sources in 4FGL catalog. The white diamond and cyan plus show the position of 4FGL J1910.2+0904c (W49A) and W49B, respectively. The red circle shows an extended γ -ray emission in 4FGL catalog, which is suggested to be associated with SNR G42.8+0.6 in 4FGL catalog. Two new point source not included in 4FGL are marked by the green crosses. Right: the SED of 4FGL J1910.2+0904c. The arrows indicating 95% upper limits, and the TS value for each energy bin is shown as the gray histogram.

Following the analysis procedure in Xin et al. [14], the energy range was divided into two parts: 1 GeV - 20 GeV and 20 GeV - 1 TeV. For each energy range, we refit the position of 4FGL J1910.2+0904c with *fermipy*, a PYTHON package that automates analyses with the Fermi Science Tools [15]. In the energy range of 1 GeV - 20 GeV, the coordinate of 4FGL J1910.2+0904c is fitted

to be (R.A.= $287.545^\circ \pm 0.013^\circ$, Dec.= $9.111^\circ \pm 0.014^\circ$), which is consistent with the result in 20 GeV - 1 TeV (R.A.= $287.553^\circ \pm 0.011^\circ$, Dec.= $9.077^\circ \pm 0.012^\circ$). Therefore, we can not determine whether the spectra upturn is caused by two individual sources or not. The left panel of Figure 2 shows the significant γ -ray emission around W49A with the energy above 20 GeV. And the γ -ray morphology is consistent with the infrared emission of W49A [16].

For the separate spectral analysis, the γ -ray emission in 1 GeV - 20 GeV band can well be fitted by a power-law model. The spectral index and photon flux are fitted to be 2.38 ± 0.14 and $(3.23 \pm 0.49) \times 10^{-10} \text{ ph cm}^{-2} \text{ s}^{-1}$, respectively. Unlike the soft spectrum in 1 GeV - 20 GeV, the spectrum in 20 GeV - 1 TeV is hard with a power-law spectral index of 1.64 ± 0.26 . And the corresponding photon flux is calculated to be $(5.49 \pm 1.47) \times 10^{-11} \text{ ph cm}^{-2} \text{ s}^{-1}$. To derive the γ -ray SEDs in the different energy ranges, six equal logarithmic energy bins are divided for the data in 1 GeV - 20 GeV and 20 GeV - 1 TeV, respectively. And the likelihood method with the best-fit position of W49A is used for each energy bin. The 95% upper limit is calculated for the bin with the TS value of W49A lower than 4.0. The resulting SED of W49A is shown in the right panel of Figure 2, together with the global spectra in the different energy ranges. The flux of the hard spectra component of W49A is above the detection sensitivity of Cherenkov Telescope Array in the north hemisphere (CTA-North; [17]), and also approach that of the Large High Altitude Air Shower Observatory (LHAASO; [18]). Therefore, the further observations by CTA-North or LHAASO will clear the γ -ray characteristics of W49A.

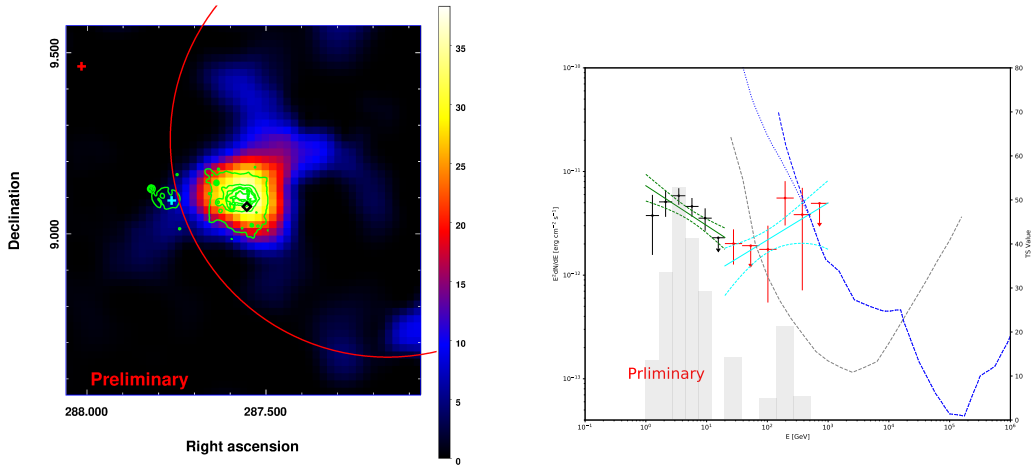


Figure 2: Left: TS map for a region of $1.0^\circ \times 1.0^\circ$ above 20 GeV. The black diamond shows the best-fit position of W49A. And the infrared emissions are marked by the green contours. Right: the SED of W49A. The black and red dots depict the results of *Fermi*-LAT data in the energy range of 1 GeV - 20 GeV and 20 GeV - 1 TeV, respectively. The global best-fitting power-law spectra with 1σ statistic errors are shown as the green and cyan butterflies. The gray histogram shows the TS value for each energy bin. The blue dotted and dotted-dashed lines represent the differential sensitivities of LHAASO (1 yr) with different sizes of photomultiplier tube (PMT)[18]. And the black dotted line shows the differential sensitivity of CTA-North (50 hr)[17].

Acknowledgments

This work is supported by the Fundamental Research Funds for the Central Universities (No. 2682021CX073, No. 2682021CX074), and the Natural Science Foundation for Young Scholars of Jiangsu Province, China (No. BK20191109).

References

- [1] Bykov, A. M. 2001, *Space Science Reviews*, 99, 317.
- [2] Aharonian, F., Yang, R., & de Oña Wilhelmi, E. 2019, *Nature Astronomy*, 3, 561.
- [3] Ackermann, M., Ajello, M., Allafort, A., et al. 2011, *Science*, 334, 1103.
- [4] Abramowski, A., Acero, F., Aharonian, F., et al. 2012, *A&A*, 537, A114.
- [5] Yang, R.-. zhi . & Aharonian, F. 2017, *A&A*, 600, A107.
- [6] Zhu, H., Tian, W. W., & Zuo, P. 2014, *ApJ*, 793, 95.
- [7] Abdo, A. A., Ackermann, M., Ajello, M., et al. 2010, *ApJ*, 722, 1303.
- [8] H. E. S. S. Collaboration, Abdalla, H., Abramowski, A., et al. 2018, *A&A*, 612, A5.
- [9] Smith, N., Whitney, B. A., Conti, P. S., et al. 2009, *MNRAS*, 399, 952.
- [10] Brogan, C. L. & Troland, T. H. 2001, *ApJ*, 550, 799.
- [11] Conti, P. S. & Blum, R. D. 2002, *ApJ*, 564, 827.
- [12] Zhang, B., Reid, M. J., Menten, K. M., et al. 2013, *ApJ*, 775, 79.
- [13] Abdollahi, S., Acero, F., Ackermann, M., et al. 2020, *ApJS*, 247, 33.
- [14] Xin, Y.-L., Liao, N.-H., Guo, X.-L., et al. 2018, *ApJ*, 867, 55.
- [15] Wood, M., Caputo, R., Charles, E., et al. 2017, 35th International Cosmic Ray Conference (ICRC2017), 301, 824
- [16] Peng, T.-C., Wyrowski, F., van der Tak, F. F. S., et al. 2010, *A&A*, 520, A84.
- [17] Cherenkov Telescope Array Consortium, Acharya, B. S., Agudo, I., et al. 2019, *Science with the Cherenkov Telescope Array*. Edited by CTA Consortium. Published by World Scientific Publishing Co. Pte. Ltd., . ISBN #9789813270091.
- [18] Bai, X., Bi, B. Y., Bi, X. J., et al. 2019, arXiv:1905.02773